EVALUATING DESIGN GUIDANCE FOR INTUMESCENT FIRE PROTECTION OF CONCRETE FILLED STEEL HOLLOW SECTIONS

8th International Conference on Structures in Fire
Shanghai, China, June 11-13, 2014

EVALUATING DESIGN GUIDANCE FOR INTUMESCENT FIRE PROTECTION OF CONCRETE FILLED STEEL HOLLOW SECTIONS

David Rush*, Luke Bisby*, and Allan Jowsey**

* BRE Centre for Fire Safety Engineering, University of Edinburgh, Edinburgh, UK
e-mails: d.rush@ed.ac.uk, luke.bisby@ed.ac.uk

** International Paint Ltd, AkzoNobel, Newcastle, UK
e-mail: allan.jowsey@akzonobel.com

Keywords: Composite columns, intumescent fire protection, forensic analysis, section factor, design.

Abstract. *Design of intumescent protection systems for concrete filled structural steel hollow (CFS) sections in the UK typically requires three input parameters: (1) a required fire resistance rating; (2) an 'effective' section factor; and (3) a limiting steel temperature for the hollow section. While the first of these is generally prescribed in building codes, the latter two require engineering judgement. This paper examines results from furnace tests on 21 CFS sections, 12 of which were protected with intumescent coatings by applying current UK design guidance. The protected sections demonstrate highly conservative fire protection under standard fire exposure; this is not typically observed for protected unfilled steel sections. Possible causes of the observed conservatism are discussed. It is demonstrated that the assumptions used in design guidance to calculate the effective section factor for protected CFS columns are physically unrealistic and inaccurate. Interim design guidance is given.*

1 INTRODUCTION

Concrete filled steel hollow structural sections (CFS) are increasingly specified in the design of multi-storey buildings; these often require structural fire resistance (F.R.) ratings of two hours or more. CFS sections may provide adequate fire resistance without the need for applied fire protection due to load sharing between the steel tube and concrete core. However in some cases available design guidance [e.g. 1] may show that adequate fire resistance cannot be achieved without protection; in these cases external fire protection must be applied, and in the UK the preferred method is intumescent coatings. In practice, design of intumescent fire protection systems for CFS sections is difficult for three reasons: (1) there is a paucity of test data on the performance of intumescent coatings when applied on CFS sections; (2) quantifiably observing the comparatively complex thermal response intumescent coatings during fire resistance tests in furnaces is difficult; and (3) fundamental differences exist between the thermal gradients in unfilled and filled hollow sections. This paper assesses current UK fire resistant design guidance for intumescent fire protection systems applied on CFS sections and identifies causes of conservative outcomes observed in a series of furnace tests on protected and unprotected CFS columns.

2 SPECIFICATION OF INTUMESCENT COATINGS FOR CFS SECTIONS

Intumescent protection (i.e. design DFTs) of structural steel is typically performed using three input parameters: (1) the required F.R.; (2) a *section factor,* the ratio of the section's heated perimeter, H_p, to its cross sectional area, A; and (3) the assumed steel *limiting temperature* (usually 520°C). These are used in conjunction with empirically determined, product specific, design tables to determine the required coating

DFT. The product specific design tables are highly optimised, based on many large scale furnace tests on *plain* structural steel sections (i.e. not CFS's) with various H_p/A and DFTs values.

To apply existing DFT tables for protection of CFS sections an 'effective' section factor, H_p/A_{eff}, is needed; this must incorporate the effect(s) of the concrete infill on the heating rates of the steel and on the load bearing capacity of the composite column. Equation 1 gives the current UK approach to determining the effective section factor for CFS sections. Equation 1 treats the problem by using DFT design guidance developed for unfilled steel sections but adds an 'equivalent' steel wall thickness, t_{ce}, which is dependent on the internal breadth of the section, b_i, and fire resistance time, t_{FR}, to the existing steel wall thickness, t_s, to account for the so-called 'thermal sink' effects of the concrete core, decreasing the effective H_p/A:

$$\frac{H_p}{A_{eff}} = \frac{1000}{t_{se}} = \frac{1000}{t_s + t_{ce}} \qquad \text{where} \qquad t_{ce} = \begin{cases} 0.15 b_i, & b_i < 12\sqrt{t_{FR}} \\ 1.8\sqrt{t_{FR}}, & b_i \geq 12\sqrt{t_{FR}} \end{cases} \tag{1}$$

This approach is physically unrealistic and potentially flawed on a number of grounds. Neither the physical rationale nor the theoretical or empirical bases for t_{ce} are reported in the literature. A key objective of the research presented herein was to validate (or otherwise) this approach.

3 FURNACE TESTS ON UNPROTECTED AND PROTECTED CFS SECTIONS

Twenty-one circular CFS columns, 12 protected and 9 unprotected, were exposed to the ISO-834 [2] standard fire in a fire testing furnace for 120 minutes (in most cases), see Table 1. The DFTs for the 12 protected CFS sections were prescribed using effective H_p/A_{eff} values given by Equation 1 with a presumed limiting steel temperature of 520°C and a required F.R. of 90 minutes. One specimen was designed to a F.R. of 75 minutes (but tested for 120 minutes) and one was protected for 120 minutes F.R. (but tested for 180 minutes). A typical test specimen is shown in Figure 1.

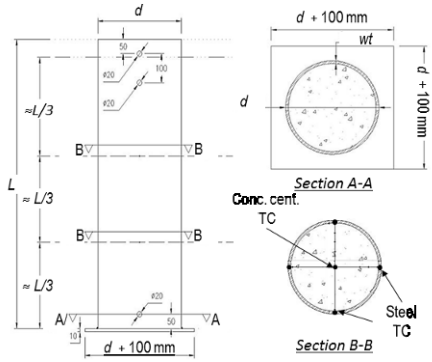

Figure 1: Specimen schematic layout

Temperatures were recorded at two heights during testing, as shown in Figure 1. Nineteen of the tests were conducted in a full scale floor furnace whereas tests 20 and 21 were conducted in a smaller cube furnace. All specimens were constructed from Grade S355 steel sections and filled with a hybrid steel and polypropylene (PP) fibre reinforced concrete mix incorporating 40 kg/m^3 and 2 kg/m^3 of steel and PP fibres, respectively, with a compressive strength of between 46.1 and 59.4 MPa and a moisture content between 3% and 6% by mass at the time of testing. Full details of the tests are presented in [3].

4 RESULTS AND DISCUSSION

Table 1 shows the average steel tube (θ_s) and concrete core ($\theta_{c.cent}$) temperatures observed at 90 minutes and 120 minutes during testing. Figure 2 shows the average, maximum, and minimum observed

steel temperatures, θ_s, for all unprotected and protected tests (excluding tests 20 and 21). The data show that: (a) the observed steel temperatures in the protected sections are well below (often by > 300°C) the target design limiting temperature of 520°C at the required F.R. time; (b) the limiting temperature of 520°C was reached in only tests 20 and 21, and in both cases this occurred more than 30 minutes after the required F.R.; (c) the temperature difference between the steel tube and the concrete core was greater in unprotected sections than in those with protection; and (d) the size of the concrete core affects the temperatures observed within the steel tube; lower steel temperatures are observed with larger cores.

Table 1: Specimen details and average temperatures recorded at 90 and 120 minutes of fire exposure.

	No.	Size (d) (mm)	Wall thickness (mm)	Length (L) (mm)	F.R. (mins)	H_p/A_{eff} (m^{-1})	DFT (mm)	θ_s (°C) 90 mins	θ_s (°C) 120 mins	$\theta_{c.cent}$ (°C) 90 mins	$\theta_{c.cent}$ (°C) 120 mins
Unprotected	1	323.9Ø	10	1000	N/A			875	949	121	132
	2	323.9Ø	8	1000				862	931	119	134
	3	219.1Ø	10	1400				902	981	193	377
	4	219.1Ø	8	1400				887	971	180	330
	5	219.1Ø	5	1400				889	973	178	331
	6	139.7Ø	10	1400				944	1005	684	844
	7	139.7Ø	8	1400				925	991	737	882
	8	139.7Ø (a)	5	1400				926	997	564	756
	9	139.7Ø (b)	5	1400				927	996	574	754
Protected	10	323.9Ø (a)	10	1000	90	40	3.5	204	244	60	86
	11	323.9Ø (b)	10	1000	90	40	3.6	206	246	57	80
	12	323.9Ø	8	1000	90	42	3.48	202	238	54	76
	13	219.1Ø	10	1400	90	39	3.55	210	254	107	142
	14	219.1Ø	8	1400	90	41	3.5	204	275	114	136
	15	219.1Ø	5	1400	90	46	3.5	230	283	109	147
	16	139.7Ø	10	1400	90	44	3.53	247	320	140	170
	17	139.7Ø	8	1400	90	46	3.52	259	350	180	254
	18	139.7Ø	5	1400	90	50	3.53	264	366	137	169
	19	139.7Ø	5	1400	90	50	3.51	234	311	141	166
	20	139.7Ø	5	1400	75	52	2	461	603 [a]	179	326
	21	139.7Ø	5	1400	120	47	4.06	270	387 [b]	151	192

[a] 520°C at 106 minutes; [b] 520°C at 155 minutes and 611°C at 180 minutes

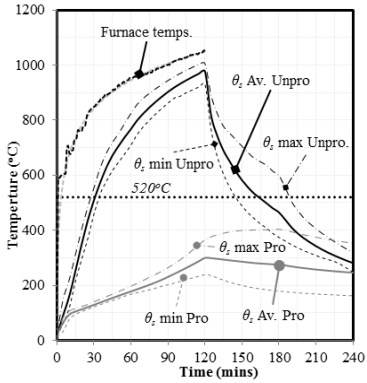

Figure 2: Unprotected and protected steel tube emperatures for CFS sections observed in furnace tests.

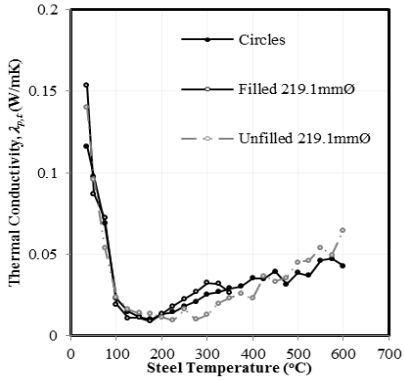

Figure 3: The intumescent variable $\lambda_{p,t}$ on filled (tests herein) and unfilled (data from industry partner) CFSs.

It is clear from Figure 2 and Table 1 that use of current guidance and DFT design data from unfilled sections to prescribe DFTs for CFS sections results in conservative steel temperatures in furnace tests. Thus, if current guidance is used to prescribe DFTs for CFS sections excessive fire protection will be applied; whilst conservative this is non optimal. The conservatism could be caused by: (1) inherently conservative DFTs in the tabulated data from unfilled section tests; (2) changes in the response, and thus the effective thermal conductivity, of the intumescent coatings when applied to sections with different thermal masses; or (3) incorrect or unrealistic calculation of H_p/A_{eff} for CFS sections.

4.1 Conservative DFT tabulated data

Available product specific tabulated DFTs are highly optimised for protecting plain steel sections. Furnace tests have shown that in most cases the designed limiting temperatures upon which the DFTs for design are based are typically reached at, or shortly after, the required F.R. times for protected unfilled sections. For instance, a 219 × 16 mm Ø circular hollow section designed for fire resistances of 90 minutes reached a limiting temperature of 520°C, at 92 minutes. Inherently conservative design tables for the plain steel sections are not considered likely to be the cause of the conservatism observed in Figure 2.

4.2 Variable thermal conductivity of protection

The variable effective thermal conductivity of the intumescent protection was assessed according to guidance given in BS EN 13381-8 [4] to investigate whether the observed conservatism in Figure 2 is due to changes in the response of the coating, for substrates of significantly different thermal mass:

$$\lambda_{p,t} = d_p \cdot \frac{A_{eff}}{H_p} \cdot c_s \cdot \rho_s \cdot \left(\frac{1}{(\theta_t - \theta_{s,t}) \cdot \Delta t} \right) \cdot \Delta\theta_{s,t} \qquad (2)$$

$\lambda_{p,t}$ is the variable effective thermal conductivity; d_p is the protection DFT; A_{eff}/H_p is the inverse of the calculated effective section factor, H_p/A_{eff}; c_s and ρ_s are the specific heat capacity and density of steel, respectively; θ_t is the furnace temperature; $\theta_{s,t}$ is the steel tube temperature; Δt is the analysis time step; and $\Delta\theta_{s,t}$ is the change in steel tube temperature during a time step. Figure 3 shows the calculated variable effective thermal conductivity, $\lambda_{p,t}$ (Eq. 2), for the same intumescent protection coating on all of the protected CFS circular sections (tests 10 to 21); for the protected 219.1 mm Ø *filled* CFS sections (tests 13 to 15); and for *unfilled* 219.1 mm Ø tubes. This shows that increasing the thermal mass of the CFS by

filling with concrete has no obvious impact on the variable insulating response of the coating, and therefore that the conservatism seen in Figure 2 is unlikely to be a result of Cause (2) postulated above.

4.3 'Effective' section factors for CFS sections

To assess the hypothesis that calculation of the effective section factor for CFS sections based on Eq. 1 is flawed, and to determine whether improvements can be made, the development of the current H_p/A_{eff} guidance (Eq. 1) must be examined.

4.3.1 Development of current guidance

Edwards [5] developed the existing H_p/A_{eff} guidance (Eq. 1 [6]) with three assumptions: (1) CFS sections can be treated as hollow steel tubes in which the concrete core provides an equivalent additional thickness of steel wall, using an empirical equation based on its required fire resistance time; (2) the effective section factor for unprotected CFS sections can be determined in the same manner as protected CFS sections as for protected versus unprotected unfilled sections; and (3) the increase in steel temperature for an unprotected steel hollow section, or CFS section using effective properties, can be calculated using an energy balance equation given in BS EN 1993-1-2 [7]:

$$\Delta\theta_{s,t} = \frac{\dot{h}_{net}}{c_s \cdot \rho_s} \cdot \frac{H_p}{A} \cdot \Delta t \tag{3}$$

The increase in steel temperatures, $\Delta\theta_{s,t}$, during a time interval, Δt, is determined based on the section factor, H_p/A, the net heat flux, $\dot{h}_{net}$, and the thermal capacity of the steel, $c_s \cdot \rho_s$. Edwards [5] used data from six standard furnace tests on unprotected CFS columns to determine an *instantaneous* effective section factor, H_p/A_{eff} *(exp)*, at each instant in time by rearranging Eq. 3, giving:

$$\frac{H_p}{A_{eff}}(\exp) = \frac{\Delta\theta_{s,t} \cdot c_s \cdot \rho_s}{\dot{h}_{net} \cdot \Delta t} \tag{4}$$

The density of steel is taken as ρ_s = 7850 kg/m^3, and the specific heat of steel is taken as c_s = 473 + 20.1· (θ_s/100) + 3.81· (θ_s/100) up to a temperature of 800°C, after which a constant value of 877.6 J/kg·K [5]. Edwards [5] uses the BS EN 1991-1-2 [8] method for calculating $\dot{h}_{net}$, where the net heat flux is the sum of the radiative and convective fluxes. Importantly, a resultant emissivity of 0.32 is assumed [5].

From test data it was determined that the instantaneous effective section factor, H_p/A_{eff} *(exp)*, varied with time during a furnace test. This is in contrast with unfilled steel sections in which the section factor remains constant due to the high thermal conductivity of steel which yields a nearly uniform temperature profile throughout the section. Using the calculated H_p/A_{eff} *(exp)*, Edwards [5] calculated the apparent instantaneous thickness of the steel tube, t_{se}, and thus the apparent effective increase in the steel tube thickness resulting from the concrete core, t_{ce}; how this led to Eq. 1 is not clear.

4.3.2 H_p/A_{eff} *(exp)* for unprotected CFS sections

Using Edwards' process [5] it is possible to calculate the instantaneous H_p/A_{eff} *(exp)* for the 12 unprotected CFS sections of the current study listed in Table 1. To calculate H_p/A_{eff} *(exp)*, an experimental net heat flux is required. A separate finite element heat transfer analysis on the unprotected CFS sections in Table 1 [3] determined that an assumed furnace emissivity of 0.38, along with a temperature dependent emissivity of steel (from [9]) were needed to properly model the temperatures experienced during the tests. The resultant emissivity thus varied with temperature between 0.08 for steel temperatures of 20-350°C, increasing to 0.25 at 565°C, and being constant at 0.25 above 565°C. The temperature dependent specific heat capacity of steel was assumed based on BS EN 1993-1-2 [7].

Figure 4(a) shows a comparison of calculated instantaneous H_p/A_{eff} *(exp)* using Eq. 5 and Edwards' [5] theoretical H_p/A_{eff} *(Th)* (Eq. 1) for a typical unprotected CFS section (Test 4). It is noteworthy that: (1) the mild peak highlighted with a data marker in the H_p/A_{eff} *(exp)* curve coincides with a phase change in the

steel at 735°C; and (2) the considerable variability in calculated instantaneous H_p/A_{eff} *(exp)* during the first 30 minutes of heating is due to the imperfect, variable control of furnace temperatures.

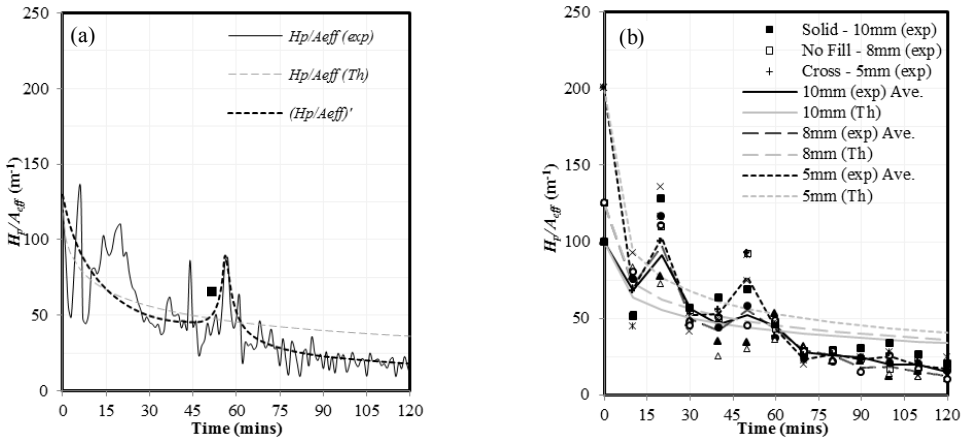

Figure 4: Instantaneous H_p/A_{eff} *(exp)* and Edwards' [10] effective H_p/A_{eff} *(Th)* for (a) a representative section (test no. 4) and (b) for all unprotected tests listed in Table 1, with data partitioned by steel wall thickness.

Figure 4(b) shows the instantaneous H_p/A_{eff} *(exp)* values calculated at 10 minute intervals throughout the tests, and shows that the instantaneous H_p/A_{eff} *(exp)* values are generally slightly lower at a given fire exposure time than Edwards' H_p/A_{eff} *(Th)*. Figure 4(b) also shows that the 'effective' contribution of the concrete core varies with time, due to the steep thermal gradients in the unprotected CFS sections that would not exist in hollow steel tubes. Larger concrete cores will have more pronounced thermal gradients that persist for longer durations of fire exposure; the contribution of the core thus also depends on its size – a factor that Edwards' guidance fails to account for.

4.3.3 Concrete core size and theoretical effective H_p/A_{eff} values

To calculate the instantaneous H_p/A_{eff} for unprotected CFS sections in a physically realistic manner the effect of the concrete thermal gradients and core size need to be incorporated. Equation 5 proposes a new method to calculate the instantaneous section factor, $(H_p/A_{eff})'$, by converting the concrete core into an equivalent *area* of steel based on the size of the core, A_c, the ratio of the respective heat capacities of concrete and steel, and an empirically determined concrete core efficiency factor, η. Using the instantaneous H_p/A_{eff} *(exp)* calculated from the tests in Table 1 as inputs for Eq. 5 (i.e. H_p/A_{eff} *(exp)* = $(H_p/A_{eff})'$), values of the core efficiency factor, η, can be calculated during each time interval as follows:

$$\left(\frac{H_p}{A_{eff}}\right)' = \frac{H_p}{A_s + \eta \cdot \left[(c_c \cdot \rho_c)/(c_s \cdot \rho_s)\right] \cdot A_c} \tag{5}$$

In the above equation c_c = 1000 J/kg°C , ρ_c = 2300 kg/m^3, c_s is the temperature dependent relationship described in Section 3.3.1 (4) of EC4 [1] to account for the phase change in steel, and ρ_s = 7850 kg/m^3. Figure 5(a) plots η against fire exposure time, t_{furn}, for all unprotected sections in Table 1. The relationship between η and the furnace time, t_{furn}, is approximately linear; however with considerable variability due to the measured steel and furnace temperature change being small and measured with a resolution of 1°C at 60 second intervals. If it is assumed that the relationship between η and fire exposure time, t_{furn}, is linear, then a larger gradient of η/t_{furn} is found for smaller internal breadths of concrete, as expected given that smaller cores have less thermal mass and will heat up more rapidly. The internal breadth, b_i, of a CFS

section can therefore be compared to the gradient η/t_{furn}, as shown in Figure 5(b) to give a relationship for η/t_{furn} for circular sections based on the internal breadth of the concrete core.

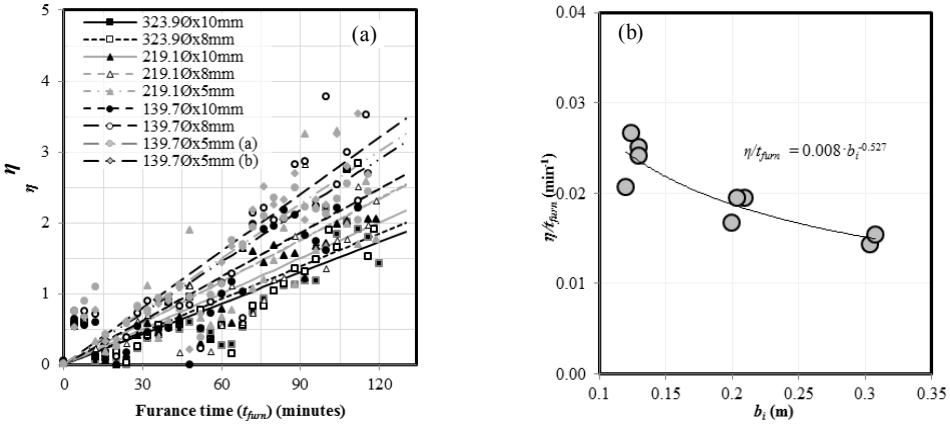

Figure 5: (a) Variation of core efficiency factor, η, with furnace exposure time, t_{furn}, for an assumed linear relationship; and (b) relationship of η/t_{furn} to b_i.

Instantaneous theoretical (H_p/A_{eff})' values can then be calculated with respect to time using η values calculated from Eq. 6 (below), with an iterative process involving calculation of the change in steel temperature using Eq. 3. Figure 4(a) compares the variation of both the instantaneous (H_p/A_{eff})', H_p/A_{eff} (Th) (Eq. 1), to the instantaneous H_p/A_{eff} (exp) calculated from Test 4 data (Eq. 4) with time; this shows that the instantaneous (H_p/A_{eff})' is an accurate and more realistic predictor of the instantaneous H_p/A_{eff} (exp). It is noteworthy that the instantaneous (H_p/A_{eff})' at 60 minutes is counter intuitively higher than the value at 45 minutes due to a peak caused by the phase change in steel at about 735°C.

η can be expressed in terms of the internal breadth, b_i, and time of furnace exposure, t_{furn}, as:

$$\eta = 0.0080 \cdot b_i^{-0.527} \cdot t_{furn} \tag{6}$$

4.2.4 Instantaneous (H_p/A_{eff})' and design

The instantaneous (H_p/A_{eff})' calculation (Eq. 5) is a superior predictor of the observed instantaneous effective section factor for unprotected CFS sections during furnace exposure. However, (H_p/A_{eff})' only calculates the effective section factor values at one specific instant in time, and does not account for the full time history effect of the concrete on the overall heat transfer. The temperatures experienced by the steel tube of an unprotected CFS result from cumulative heating where the (H_p/A_{eff})' varies with time. Calculating steel temperatures using a single instantaneous (H_p/A_{eff})' over a period of time will result in unconservative steel temperatures and thus under-predict the amount of protection required. It is thus inappropriate to use a single instantaneous value of (H_p/A_{eff})' to calculate either the steel temperature after a given length of time or the required DFT for protection.

However, specifying intumescent coating thicknesses from tabulated DFT data requires a single effective section factor. A single time-averaged effective section factor, $(H_p/A_{eff})'_{t.ave}$, that accounts for the cumulative heating of a CFS section resulting from time dependent instantaneous (H_p/A_{eff})' values (Eq. 5) must therefore be found. This must result in the same steel tube temperature when used in Eq. 3 as would be found if using the variable time dependent instantaneous (H_p/A_{eff})' values for a specific fire resistance time. By calculating $(H_p/A_{eff})'_{t.ave}$ for a series of fire resistance times, a trace of the time-averaged effective section factor, $(H_p/A_{eff})'_{t.ave}$, can be created (Figure 6(a)) for a representative unprotected test.

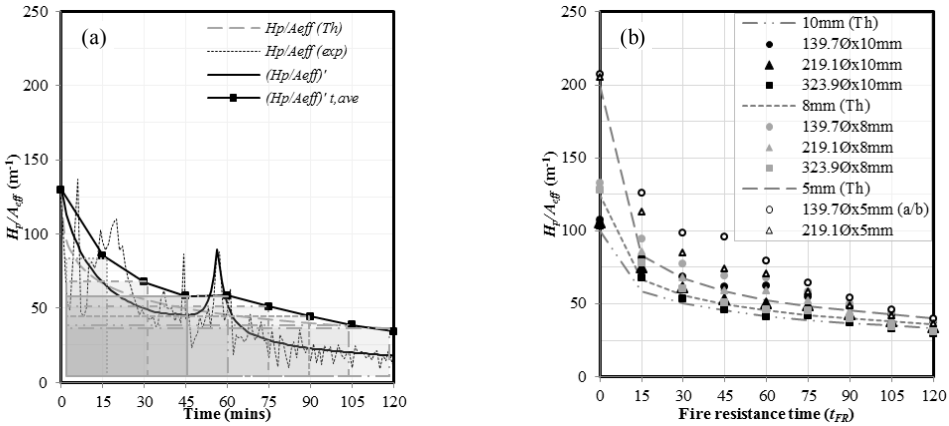

Figure 6: (a) representative comparison of $(H_p/A_{eff})'$, $H_p/A_{eff}\,(exp)$, $H_p/A_{eff}\,(Th)$, and $(H_p/A_{eff})'_{t.ave}$, (219.1Øx8mm); and (b) comparison of $H_p/A_{eff}\,(Th)$ and $(H_p/A_{eff})'_{t.ave}$, for unprotected tests presented herein.

Figure 6(b) compares $(H_p/A_{eff})'_{t.ave}$ to the current effective section factor guidance $H_p/A_{eff}\ (Th)$ values with time of fire exposure for all unprotected CFS sections in the current study, and shows that the $(H_p/A_{eff})'_{t.ave}$ values are generally greater than the $H_p/A_{eff}\ (Th)$ values at the same fire resistance time. Therefore, if the time-averaged $(H_p/A_{eff})'_{t.ave}$ values for the unprotected CFS sections are used a thicker DFT would be prescribed. Whilst the new time-averaged $(H_p/A_{eff})'_{t.ave}$ values may be more physically realistic than Edwards' approach, they appear not to address the observed conservatism in furnace tests.

Fundamental changes exist in the thermal gradients within protected CFS sections compared unprotected sections. Protected sections experience a less severe thermal gradient within the core, which effectively increases the effect that the concrete core has on the effective section factor. The thermal gradient within a protected section depends on the heating rate of the steel, which is affected by: (1) the limiting temperature to which the steel is protected – higher limiting temperatures result in more severe thermal gradients reducing the effect(s) of the concrete core; (2) the required F.R. – longer F.R. produces shallower thermal gradients, increasing the effect(s) of the concrete core; and (3) the intumescent coating performance, especially its variable effective thermal conductivity and physical charring characteristics.

Additional analytical and experimental work on protected CFS sections is needed to avoid the inherent conservatisms in the current approach for the specification of intumescent protection CFS sections, so that the effective section factor for protected CFS sections is better understood and a more rational method developed. For the time being, the authors recommend that current guidance from Eq. 1 [6] be used to determine the effective section factor for CFS columns, since the testing and analysis presented herein show this approach to be conservative.

11 CONCLUSION

This paper has presented results from standard furnace tests on 12 unprotected and 14 intumescent fire protected CFS sections. The following conclusions can be drawn:

- The current method of prescribing intumescent coating DFTs for CFS sections is overly conservative.
- This paper has proposed a more physically realistic instantaneous effective section factor model for unprotected CFS sections, incorporating the effects of the size of the section and the required fire resistance time. However, the new method is even more conservative for protected CFS columns.
- The observed conservatism in the current UK approach to specifying design DFTs results from the inappropriate application of unprotected CFS effective section factors for prescribing intumescent

coatings on protected CFS sections. Until a more rational method for determining the effective section factors for protected CFS sections is developed the current guidance [6] should be used.

REFERENCES

[1] CEN, "BS EN 1994-1-2: Eurocode 4: Design of composite steel and concrete structures; Part 1-2: Structural Fire Design," Brussels, Belgium, 2005.

[2] ISO, "ISO 834: Fire resistance tests-elements of building construction," Geneva, Switzerland, 1999.

[3] D. Rush, "Fire performance of unprotected and protected concrete filled structural hollow sections," University of Edinburgh, 2013.

[4] CEN, "BS EN 13381-8:2010: Test methods for determining the contribution to the fire reistance of structural members; Part 8: Applied reactive protection to steel members," Brussels, Belgium, 2010.

[5] M. Edwards, "Reinstatment of concrete filled structural hollow section columns after short duration fires - Phase 2: Standard fire tests on full size columns.," Corby, Northants, 1998.

[6] S. J. Hicks, G. M. Newman, M. Edwards, and A. Orton, "Design guide for concrete filled columns," Corus Tubes, Corby, Northants, 2002.

[7] CEN, "BS EN 1993-1-2:2005: Eurocode 3: Design of steel stuctures; Part 1-2: General rules - Structural fire design," Brussels, Belgium, 2009.

[8] CEN, "BS EN 1991-1-2: Eurocode 1: Actions on structures; Part 1-2: General Actions - Actions on structures exposed to fire," Brussels, Belgium, 2009.

[9] T. Paloposki and L. Liedquist, *Steel emissivity at high temperatures - Research notes*. Tampere, Finland: Technical Research Centre of Finland, 2005.